



Deposited via The University of Leeds.

White Rose Research Online URL for this paper:

<https://eprints.whiterose.ac.uk/id/eprint/236743/>

Version: Accepted Version

Article:

Tan, Z., Ma, X., Lu, K. et al. (2026) Governing atmospheric oxidation capacity is the key to synergistic air quality and climate gains. *One Earth*, 9 (1). 101569. ISSN: 2590-3330

<https://doi.org/10.1016/j.oneear.2025.101569>

This is an author produced version of an article published in *One Earth*, made available via the University of Leeds Research Outputs Policy under the terms of the Creative Commons Attribution License (CC-BY), which permits unrestricted use, distribution and reproduction in any medium, provided the original work is properly cited.

Reuse

This article is distributed under the terms of the Creative Commons Attribution (CC BY) licence. This licence allows you to distribute, remix, tweak, and build upon the work, even commercially, as long as you credit the authors for the original work. More information and the full terms of the licence here:
<https://creativecommons.org/licenses/>

Takedown

If you consider content in White Rose Research Online to be in breach of UK law, please notify us by emailing eprints@whiterose.ac.uk including the URL of the record and the reason for the withdrawal request.



Governing Atmospheric Oxidation Capacity as the Key to Synergistic Air Quality and Climate Gains

Zhaofeng Tan^{1#}, Xuefei Ma^{1#}, Keding Lu^{1*}, Xuan Li¹, Qindan Zhu², Franz Rohrer³, Anna Novelli³, Hendrik Fuchs^{3, 4}, Andreas Wahner³, Lisa Whalley⁵, Dwayne Heard⁵, Steven Brown^{6,7}, Xin Zhang⁸, Yuanhang Zhang^{1*}

¹ State Key Laboratory of Regional Environment and Sustainability, State Environmental Key Lab for Ozone Pollution Control, College of Environmental Sciences and Engineering, Peking University, Beijing, China

² Department of Earth, Atmospheric and Planetary sciences, Massachusetts Institute of Technology, USA

³ Institute of Energy and Climate Research, IEK-8: Troposphere, Forschungszentrum Jülich GmbH, Jülich, Germany

⁴ Department of Physics, University of Cologne, Cologne, Germany

⁵ School of Chemistry, University of Leeds, Leeds, LS2 9JT, UK

⁶ NOAA Chemical Sciences Laboratory, Boulder, CO, USA

⁷ Department of Chemistry, University of Colorado, Boulder, CO, USA

⁸ Global Nitrogen Innovation Center for Clean Energy and Environment, University of Maryland Center for Environmental Science, USA

These authors contributed equally to this work.

Correspondence: k.lu@pku.edu.cn (K.D.L.), yhzhang@pku.edu.cn (Y.H.Z.)

Lead contact: Keding Lu (k.lu@pku.edu.cn)

SUMMARY

Effective management of air quality and climate change requires recognition of their fundamental coupling through atmospheric oxidation capacity (AOC), which governs the atmosphere's self-cleansing capacity. However, policies often overlook the nonlinear chemical feedbacks inherent to AOC, leading to fragmented strategies that risk unintended consequences. Here we demonstrate that uncoordinated strategies, such as reducing fossil fuel-related NO_x without concurrent methane controls, can suppress OH radicals, inadvertently prolonging methane's lifetime. This "chemical lockdown paradox", observed during COVID-19 lockdowns, reveals critical trade-offs, where short-term air quality gains may increase methane accumulation, offsetting the climate benefits of CO₂ abatement. Given AOC's spatial heterogeneity, such effects can extend beyond local scales. We thus propose a regulatory framework integrating AOC dynamics through coordinated multi-pollutant controls, advanced multiscale AOC monitoring, and improved Earth system models with fully-coupled chemical feedbacks. This framework paves a science-based pathway for synergistically managing air quality and climate mitigation throughout the decarbonization transition.

1 AOC: THE UNSEEN ATMOSPHERIC GOVERNOR

2 Air pollution and climate change constitute two intrinsically linked
3 environmental crises that pose severe threats to human health and ecosystem
4 security. This linkage stems from the fact that many anthropogenically emitted
5 gases and particulate matter simultaneously impact both air quality and
6 climate warming. Consequently, mitigation efforts targeting one crisis
7 inevitably influence the other. Nevertheless, conventional policy frameworks

8 have predominantly emphasized targeted reductions of specific pollutants,
9 including nitrogen oxides (NO_x), sulfur dioxide (SO_2), fine particulate matter
10 ($\text{PM}_{2.5}$), methane (CH_4), and carbon dioxide (CO_2). However, atmospheric
11 responses to such emission controls are often nonlinear and complex. A critical
12 yet often overlooked factor governing these responses is the Atmospheric
13 Oxidation Capacity (AOC), which refers to the ability of the atmosphere to
14 cleanse itself of pollutants through chemical oxidation (Figure 1). AOC plays a
15 decisive role in regulating the atmospheric lifetime of potent greenhouse gases
16 such as CH_4 ¹, while simultaneously determining the formation of secondary
17 pollutants like ozone and $\text{PM}_{2.5}$ ²⁻³, both of which are also significant climate
18 forcers. Emission reduction strategies targeting individual pollutants without
19 accounting for their interactive effects on AOC, risk triggering unintended
20 atmospheric consequences that may undermine both air quality gains and
21 climate mitigation efforts⁴⁻⁵.

22 The COVID-19 lockdowns offered a compelling real-world illustration of
23 this systemic risk. Rapid declines in transportation and industrial activity led to
24 sharp reductions in NO_x emissions, which is a common target in
25 decarbonization and clean air policies⁶⁻⁷. However, this decrease also
26 suppressed the formation of hydroxyl radical (OH), the atmosphere's primary
27 oxidant, leading to a decline in atmospheric cleansing capacity and consequent
28 accumulation of CH_4 ⁸⁻⁹. Studies indicate that the reduction in OH levels during
29 early 2020 contributed to a 53% increase in the methane growth rate anomaly⁴,
30 partially offsetting the climate benefits associated with reduced CO_2
31 emissions. This “chemical lockdown paradox” underscores a critical
32 governance challenge: effective policies must consider not only what we
33 remove from the atmosphere, but also how those removals affect the very
34 processes that sustain atmospheric health. If CH_4 accumulation outpaces AOC

35 recovery, a destabilizing “runaway” effects could occur¹⁰, potentially collapsing
36 the atmospheric self-cleansing capacity.

37 Analogous trade-offs are evident in regional air quality management. For
38 example, stringent NO_x reduction in the absence of concurrent controls on
39 volatile organic compounds (VOCs) has in some urban regions inadvertently
40 increased ozone pollution¹¹⁻¹². Likewise, efforts to reduce PM_{2.5} concentrations
41 by controlling aerosol precursors may modify photolysis rates and alter
42 oxidative pathways, in some cases raising surface ozone levels in certain
43 regions¹³⁻¹⁴. Studies suggest that a major driver of ozone increase in the North
44 China Plain was the approximately 40% reduction in PM_{2.5} between 2013-2017,
45 which slowed the aerosol sink of hydroperoxy radical (HO₂) and thereby
46 accelerated ozone production⁵. These unintended consequences highlight the
47 inherent constraints of isolated emission control strategies. To achieve
48 synergistic improvements in both ozone and PM_{2.5}, policies must be designed
49 with a holistic understanding of their combined effect on AOC.

50 The integration of AOC into air quality and climate governance is growing
51 increasingly urgent amid rapidly evolving emission policies. Although global
52 efforts to reduce fossil fuel consumption and decarbonize energy systems are
53 essential, these initiatives may profoundly reshape the atmospheric chemical
54 environment, notably altering the abundance of OH²². Effectively addressing
55 climate change and protecting air quality therefore require a nuanced,
56 systems-oriented approach centered on sustaining AOC. In this perspective, we
57 systematically evaluate the key chemical drivers and regional variations of
58 AOC, identify critical knowledge gaps in current modelling frameworks, and
59 propose an integrated framework for monitoring and governing AOC across
60 scales. By establishing AOC as a central scientific and policy nexus in
61 atmospheric and climate governance, co-designed strategies can be

62 developed, optimized, and implemented to enhance atmospheric resilience and
63 deliver dual environmental and climate benefits.

64 **CURRENT UNDERSTANDING OF TROPOSPHERIC AOC**

65 **Fundamental Chemistry and Governing Mechanisms**

66 The stability of AOC hinges on a finely tuned set of chemical reactions
67 dominated by OH radicals (Figure 1)¹⁵. These radicals are generated globally
68 via the photolysis of ozone in the presence of water vapor. Through catalytic
69 oxidation, OH radicals remove pollutants such as CH₄, CO, and VOCs, a process
70 that simultaneously produces peroxy radicals (RO₂). The resulting peroxy
71 radicals subsequently oxidize NO to NO₂, which undergoes photolysis to
72 regenerate O₃ and recycle NO, thereby sustaining the oxidative cycle. Radical
73 propagation terminates either through the reaction between OH and NO₂,
74 forming nitric acid (HNO₃), or via peroxy radical recombination, which produces
75 stable peroxides (ROOH)¹⁶. Notably, the very mechanisms responsible for
76 atmospheric cleansing also regenerate ozone and promote the formation of
77 secondary aerosols, both of which act as potent air pollutants and short-lived
78 climate forcers. Thus, the processes that maintain atmospheric self-cleansing
79 capacity are intrinsically double-edged, sustaining a delicate balance highly
80 sensitive to external perturbations.

81 AOC exhibits complex, nonlinear responses to anthropogenic emissions.
82 For example, although increased NO_x concentrations generally enhance global
83 OH production, thereby shortening the atmospheric lifetimes of CH₄ and CO,
84 changes in NO_x emissions do not consistently lead to proportional changes in
85 atmospheric concentrations due to OH-mediated feedbacks (Box 1 scenario c
86 and d)¹⁷. In contrast, reductions in CH₄ emissions directly lower its atmospheric
87 burden and decrease OH consumption, resulting in higher OH concentrations

88 (Box 1 scenario a). The behavior of CO is more complex. Although it dominates
89 global OH turnover, its atmospheric abundance arises not only from direct
90 emission but largely from CH₄ oxidation through HCHO intermediates. The
91 latter process consumes about 2.5 OH radicals per CH₄ molecule, compared to
92 only one OH per directly emitted CO molecule. As a result, CH₄ emissions exert
93 a stronger influence on the atmospheric oxidation system, owing to their
94 greater cumulative OH consumption and their role as the primary source of CO,
95 whereas CO emission perturbations have a comparatively minor effect (Box 1
96 scenario b)¹⁸. Stabilizing AOC therefore necessitates carefully balanced,
97 multi-pollutant reduction strategies (Box 1 scenario f).

98 Moreover, climate change may perturb AOC through multiple pathways.
99 Elevated temperatures and water vapor levels could enhance OH production by
100 accelerating ozone photolysis. However, this can be counteracted by the
101 temperature-dependent acceleration of CH₄ oxidation kinetics, which
102 consumes OH and may moderate the net increase in OH concentration (Box 1
103 scenario g and h). Furthermore, climate-driven increases in biogenic emissions,
104 notably N₂O, contribute to stratospheric O₃ depletion. The resulting increase in
105 tropospheric ultraviolet radiation elevates surface OH concentrations and
106 shortens the lifetime of CH₄¹⁹ (Box 1 scenario e). These interacting feedbacks
107 complicate atmospheric predictions and highlight the necessity of integrated
108 chemistry-climate assessments.

109 **Quantifying AOC: Metrics and Interpretation**

110 Quantifying AOC across scales remains a fundamental challenge, yet is
111 essential for understanding atmospheric chemistry and climate interactions.
112 Accurate quantification requires the careful selection of appropriate metrics
113 aligned with specific research objectives. From a kinetic perspective, we
114 distinguish two principal metrics: (1) the OH concentration, an intensive

115 property governing oxidative potential, and (2) the net O_3 production rate
116 ($P(O_3)$), an extensive property characterizing chemical transformation rates.
117 These complementary metrics serve distinct but interrelated roles in
118 atmospheric process analysis.

119 OH concentration provides a foundational measure of AOC, particularly on
120 larger scales. Atmospheric trace gases degradation is primarily driven by three
121 key oxidants, namely OH, O_3 , and NO_3 . OH and NO_3 radicals exhibit extremely
122 short lifetimes, typically under one minute, resulting in pronounced spatial
123 heterogeneity tied to the distribution of their precursors. Appropriate
124 spatiotemporal averaging of these radical concentrations yields a robust
125 intensive parameter that quantitatively represents AOC while inherently
126 accounting for variability. In practice, OH concentration is widely adopted as a
127 proxy due to its central role in oxidizing most trace gases. Although this
128 simplification may lead to a modest underestimation of total AOC, it provides a
129 standardized and practical framework for cross-scale comparison. For
130 long-lived species such as CH_4 , decadal-average OH concentrations provide a
131 robust measure of the atmosphere's self-cleansing capacity and remain the
132 benchmark for global AOC assessment.

133 In the context of regional air quality, metrics of prompt oxidation rate, such
134 as $P(O_3)$, offer more direct insight into secondary pollutant formation. This
135 process involves the radical-driven oxidation of primary pollutants such as NO_X ,
136 VOCs, generating intermediate species whose conversion efficiency to
137 secondary products like O_3 and SOA depends strongly on local chemical
138 conditions. Tropospheric O_3 concentrations have approximately doubled since
139 the pre-industrial era²³, suggesting a rise in $P(O_3)$ and thus an increase in AOC.
140 In contrast, Earth system models indicate that global mean OH concentrations
141 have varied by less than 10% over the same period²⁴, though uncertainties in

142 chemical mechanisms complicate these estimates²⁵. This divergence
143 underscores the need to tailor AOC definitions to the process and timescale of
144 interest. The historical rise in O₃ reflects a coupled atmospheric response,
145 where increased O₃ production from anthropogenic emissions accompanies
146 OH stabilization through NO_x-mediated HO_x cycling, illustrating a nonlinear
147 feedback within the oxidation system. Thus, P(O₃) serves as a valuable
148 diagnostic of chemical efficiency in pollutant formation, revealing aspects of
149 oxidation chemistry that are not captured by OH concentrations alone.

150 In polluted environments with high aerosol loading, AOC assessment
151 requires additional considerations. Multiphase chemistry necessitates
152 supplementary metrics, such as O_x (=O₃+NO₂) and secondary aerosol mass
153 fractions, to fully capture oxidation processes. Nevertheless, in this perspective,
154 we focus mainly on gas-phase reactions to reduce system complexity, while
155 clarifying how OH-mediated hydrocarbon oxidation couples air pollution with
156 climate change.

157 **Key Drivers and Chemical Regimes of AOC**

158 The spatial distribution of AOC is primarily governed by emission patterns,
159 with NO_x serving as the dominant driver of its variability²⁶. This regulatory role
160 manifests as a clear contrast between chemical regimes, where polluted urban
161 regions are often NO_x-saturated, suppressing oxidation efficiency, whereas
162 remote regions are typically NO_x-limited, with oxidative capacity tightly coupled
163 to NO_x availability²⁰⁻²¹. State-of-the-art box model simulations capture this
164 contrast, revealing the distinct responses of OH concentration and in-situ P(O₃)
165 to varying NO levels across urban, forest, and marine environments (Figure 2)²⁷.
166 A key feature emerging from these simulations is the divergent behavior of the
167 two AOC metrics across NO concentrations spanning six orders of magnitude.
168 OH concentrations remain relatively stable, maintaining levels between (1-5)×

169 10^6 cm^{-3} with less than fivefold variation. In contrast, $P(\text{O}_3)$ exhibits pronounced
170 nonlinearity, transitioning from slightly negative values in pristine marine air
171 (ppt NO levels, mixing ratios of parts per trillion) through maximum production
172 rates (tens of ppb/h, parts per billion per hour) in moderately polluted urban air
173 (a few ppb NO, parts per billion) to nearly zero in heavily polluted urban air (tens
174 of ppb NO).

175 Furthermore, while OH concentrations at a given NO level can differ across
176 regimes (Figure 2a), $P(\text{O}_3)$ displays a smooth, consistent functional relationship
177 with NO that is largely independent of the local environment (Figure 2b). This
178 divergence arises from regime-specific VOC characteristics, particularly their
179 abundance and chemical complexity, which modulate the conversion efficiency
180 of OH radicals to peroxy radicals. Globally, a positive feedback links O_3 and OH,
181 where VOCs oxidation drives O_3 production, which in turn photolyzes to
182 generate OH and accelerates further oxidation. In the marine boundary layer
183 (MBL), however, limited OH reactants (mainly CH_4 and CO) suppress radical
184 propagation, while extremely low NO concentrations restrict O_3 production,
185 constraining the sustainability of AOC. This establishes a fundamental spatial
186 decoupling: although the global cleansing capacity for long-lived gases like CH_4
187 is determined by moderate OH over the vast MBL, the chemical potential for O_3
188 production is concentrated over continents, particularly in urban and suburban
189 areas. The hemispheric-scale transport of O_3 , which has an atmospheric
190 lifetime of approximately one month, critically couples these chemically distinct
191 domains, enabling OH production via O_3 photolysis even in remote areas where
192 local O_3 chemistry results in net loss (e.g., through reactions with OH, HO_2 and
193 halogen species in the MBL)²⁸. This O_3 -mediated chemical buffering effectively
194 extends AOC globally, facilitating pollutant degradation even in NO_x -limited
195 environments.

196 Nevertheless, at smaller scales, the oxidation capacity is not unlimited and
197 can be exceeded under high emission loads, particularly in urban areas²⁹. When
198 local AOC recovery mechanisms are overwhelmed, excess pollutants are
199 transported downwind, moving across chemical regimes and undergoing
200 oxidation over broader spatial scales. This redistribution mechanism, which
201 links local chemistry to global AOC, represents a critical feature of atmospheric
202 self-cleansing. It underscores the necessity of multi-scale emission
203 management strategies that explicitly account for the inherent spatial
204 heterogeneity and nonlinearity of atmospheric oxidation processes.

205 **DIVERGENT AOC TRENDS AND REGIONAL POLICY**
206 **LESSONS**

207 A central question in AOC research involves determining long-term trends
208 in OH concentrations, given their critical role in regulating the removal of CH₄
209 and its associated climate impacts. Reliable quantification of OH variability is,
210 therefore, essential for understanding how anthropogenic emissions influence
211 the atmospheric lifetime and burden of CH₄. The complex variations in the
212 decadal-scale growth rate of atmospheric CH₄ underscore the urgency and
213 importance of this quantitative effort.

214 Observational records reveal that although CH₄ has generally exhibited a
215 long-term increasing trend since industrialization, this trend was interrupted by
216 a distinct pause between 2000 and 2006. While the long-term increase is
217 largely attributed to the rise in anthropogenic emissions³⁰, the causes of the
218 pause remain debated. Proposed explanations include an increase in OH
219 concentrations enhancing CH₄ oxidation, a temporary halt in CH₄ emissions
220 growth, or a combination of both³¹⁻³². Definitive attribution, however, is
221 complicated by substantial uncertainties in quantifying key processes such as

222 OH concentration estimates, wetland emissions, fossil fuel leakage, and
223 microbial sources. Specifically, each of these factors contributes approximately
224 10% uncertainty to the CH₄ budget. Cumulatively, these uncertainties exceed
225 the observed CH₄ growth rate of ~0.5% yr⁻¹, making it difficult to confidently
226 attribute both the historical pause and the subsequent renewed growth.

227 Model simulations from CESM2/WACCM6 initial-condition ensembles
228 suggest a sustained increase in global OH after the year 2000 (Figure 3)³³,
229 which may have partly attenuated CH₄ growth between 2000 and 2006, though
230 its magnitude appears insufficient to fully account for the stabilization. The
231 subsequent leveling-off of OH concentrations after 2007 coincides with the
232 resumption of CH₄ growth³⁴, reinforcing the coupling between OH variability
233 and CH₄ trends. The unprecedented acceleration in CH₄ growth during the 2020
234 COVID-19 lockdowns further illustrates how abrupt reductions in NO_x
235 emissions can perturb global OH levels, leading to a substantial increases in
236 CH₄ growth⁴, although elevated wetland emissions also contributed
237 significantly to the anomaly³⁵⁻³⁶. While this Perspective focuses on elucidating
238 the linkages between global OH concentrations and regional air pollution rather
239 than attributing specific CH₄ trends, it underscores the necessity for Earth
240 system models to adequately resolve these critical chemistry-climate
241 interactions.

242 As global OH concentrations are primarily governed by NO_x emissions and
243 ultraviolet radiation³⁷, a realistic representation of these drivers is critical for
244 projecting future OH levels and adjustments in CH₄ atmospheric lifetime.
245 Among these drivers, natural NO_x sources, particularly lightning, play a critical
246 yet poorly constrained role in the global oxidative budget⁵². These emissions
247 are strongly modulated by weather and climate, and their representation in
248 models remains a major source of uncertainty. Emerging evidence indicates

249 that lightning directly generates OH radicals alongside NO, with OH production
250 efficiencies ranging from 2% to 16%⁵³. As a key driver of wildfires and with
251 frequency projected to increase 41% by the 2090s under RCP6.0 climate
252 scenario⁵⁴, lightning constitutes one of the largest uncertainties in projecting
253 future OH levels and AOC⁵¹. The uncertainties introduced by these complex and
254 variable drivers make robust observational constraints on OH levels especially
255 critical for evaluating model simulations. However, observational constraints
256 on OH beyond 2014 remain subject to significant uncertainty, primarily due to
257 limitations of the methyl chloroform (CH₃CCl₃) tracer method, whose accuracy
258 has been severely compromised as concentrations decline below 5 pptv⁵⁰. This
259 scarcity of robust observational data after 2014 critically limits our ability to
260 evaluate model simulations and refine future projections.

261 The regional distribution of OH concentrations provide additional critical
262 insights into the atmospheric lifetime and burden of CH₄. As outlined in Section
263 2, the spatial decoupling between global OH and O₃ as AOC metrics reflects a
264 fundamental heterogeneity in oxidation intensity. This heterogeneity manifests
265 through three key mechanisms: First, tropospheric O₃ production is
266 concentrated primarily in the Northern Hemisphere mid-latitudes⁵¹, where major
267 urban and industrial regions (e.g., China, the United States, and Europe) are
268 located. NO_x emissions from these areas not only drive intense local
269 photochemistry but also help sustain OH levels in remote forested and marine
270 environments, thereby facilitating the global removal of CH₄ (Figure 2). Second,
271 the spatial heterogeneity of OH concentrations leads to a pronounced tropical
272 dominance in the oxidation of VOCs and, consequently, in atmospheric CH₄
273 consumption²⁴. Interhemispheric OH differences further modulate CH₄
274 distribution and modify the climate-chemistry interactions in response to
275 anthropogenic emissions³⁸. Third, and crucially for policy, regional-scale OH

276 variations serve as a key metric for evaluating the effectiveness of air pollution
277 mitigation strategies, which are typically implemented at national or
278 subnational scales.

279 The contrasting trends between China and the United States offer a clear
280 illustration of this principle (Figure 3). In the United States, OH concentrations
281 have declined alongside improvements in air quality³⁹. In China, by contrast, OH
282 has increased consistent with observed rise in O₃⁴⁰ and secondary aerosols⁴¹,
283 despite reductions in primary emissions following implementation of the
284 national Air Quality Action plan in 2013⁴². This divergence can be partly
285 attributed to differing NO_x reduction strategies. China's integrated approach
286 targeting both NO_x and VOC control⁴³ may help sustain regional AOC while
287 improving air quality¹⁸, whereas the predominant focus on NO_x reduction in the
288 United States⁴⁴⁻⁴⁶ contributes to a more pronounced regional OH decline. Such
289 regional-scale OH reductions, while beneficial for local air quality, may influence
290 AOC beyond local scales⁹ and introduce climate trade-offs by weakening the
291 CH₄ sink, as evidenced during the COVID-19 lockdowns⁴. Current Earth system
292 models, however, still do not fully capture these climate impacts resulting from
293 air quality-driven changes in CH₄ loss rates, despite recent efforts to
294 incorporate such chemistry-climate interactions⁴⁷⁻⁴⁹.

295 At regional and urban scales, the intricate interplay between reactive
296 nitrogen and carbon chemistry emerges as a key regulator of AOC. This
297 regulation is particularly evident in urban environments, where primary radical
298 sources such as nitrous acid (HONO) and HCHO photolysis often dominate
299 over O₃ photolysis. This dominance explains the occurrence of winter
300 photochemical smog in high-emission regions, such as areas with extensive
301 natural gas production or petrochemical industries like the Utah Basin in the
302 United States, where significant emissions of oxygenated volatile organic

303 compounds (OVOCs) drive winter O₃ pollution⁵⁶⁻⁵⁷. In China, unique topographic
304 features favor large-scale pollution accumulation, especially in the North China
305 Plain under stagnant atmospheric conditions, creating ideal environments for
306 studying these processes. Radical budget analyses based on in situ
307 measurements confirm the roles of reactive nitrogen species beyond NO_x,
308 particularly HONO and nitryl chloride (ClNO₂), in the formation of O₃ and
309 aerosols⁵⁸⁻⁵⁹.

310 Beyond these established mechanisms, the understanding of AOC is
311 further complicated by recently identified chemical processes whose impacts
312 are not yet fully constrained⁶⁰⁻⁶¹. For instance, regional fertilization via
313 agricultural activities releases HONO and N₂O, which may promote O₃
314 pollution⁶², offset pollution control measures⁶³, or alter the CH₄ lifetime through
315 troposphere-stratosphere interactions⁹. Similarly, the growing recognition of
316 reactive halogen chemistry reveals its role in urban air pollution and climate
317 change⁶⁴⁻⁶⁵, offering new insights for controlling secondary pollutants.
318 However, the chemical behavior of short-lived halogen species remains
319 inadequately characterized. Of particular interest are their indirect climatic
320 effects mediated through changes in AOC, an aspect not yet incorporated into
321 current Earth system models⁶⁶. In conclusion, these non-conventional pathways
322 significantly enhance local AOC under intensive anthropogenic emissions,
323 accelerating the formation of secondary pollutants and posing novel
324 challenges for air quality management. The resulting complexity underscores
325 that the limited understanding of emission profiles and chemical mechanisms
326 remains a major source of uncertainty in air quality prediction and regulation
327 worldwide⁶⁷.

328 The formation of secondary pollution is further complicated by seasonal
329 variations in AOC. Summer O₃ pollution is primarily driven by OH-initiated

330 oxidation pathways, whereas winter secondary aerosol formation involves both
331 gas-phase and multiphase processes⁶⁸⁻⁶⁹. Resolving these dynamics requires
332 long-term observational records of OH concentrations, which are critical for
333 identifying the factors controlling AOC across timescales from diurnal to
334 seasonal⁷⁰. The importance of such datasets is underscored by a five-year in
335 situ study, which revealed a robust correlation between OH concentrations and
336 O₃ photolysis rates ($j(O^1D)$) that persisted across diverse chemical regimes⁷¹.
337 Although geographically limited to a single rural site, these findings
338 significantly advance our understanding of AOC drivers. Furthermore,
339 decadal-scale OH measurements are essential for tracking the evolution of air
340 pollution and its associated climate feedbacks. We therefore propose
341 establishing a multi-scale observational network by employing comprehensive
342 techniques across local, regional and global scales (see Box 2). Such an
343 integrated network would greatly enhance our ability to interpret complex
344 climate-chemistry interactions through long-term, high-quality data.

345 **AN INTEGRATED AOC GOVERNANCE FRAMEWORK**

346 For future applied and scientific investigations, we propose exploring the
347 role and fate of AOC through a consolidated framework that unifies the
348 scientific and technical basis to address both air pollution and climate change,
349 consistent with existing environmental conventions (Figure 4). Future
350 atmospheric dynamics will be shaped by energy system transitions toward
351 climate mitigation targets, alongside climate-driven shifts in natural emissions,
352 including biogenic, wetland, lightning-derived sources. The nonlinear
353 atmospheric response to emissions, mediated by AOC mechanisms, exhibits
354 particular sensitivity to declining NO_x emissions, a trend expected to intensify.
355 To optimize regional air quality strategies, mitigation roadmaps must rigorously
356 account for AOC feedbacks, necessitating targeted research to strengthen the

357 scientific basis for implementing a win-win strategy that simultaneously
358 improves air pollution control and climate change mitigation. These efforts
359 must also be contextualized within the broader scope of other international
360 environmental conventions.

361 **Navigating the Energy Transitions Green Paradox**

362 The global energy transition is accelerating decarbonization across fossil
363 fuel-intensive sectors, including heavy industry, transportation, and power
364 generation. Current technological pathways for emission reduction can be
365 classified into three categories based on their impacts on atmospheric
366 chemistry: (1) the adoption of zero-emission technologies, such as
367 photovoltaics, wind, hydroelectric, and nuclear power, enables the simultaneous
368 reduction of CO₂ and NO_x emissions; (2) the shift to hydrogen (H₂) fuel cells
369 reduces CO₂ and NO_x emissions at the point of use but can be accompanied by
370 unintended release of reduced chemical species, such as fugitive H₂ emissions
371 across the supply chain; and (3) the combustion of H₂ or ammonia, as a
372 replacement for fossil fuels, reduces CO₂ emissions but may be offset by
373 elevated NO_x formation from high combustion temperature and by H₂ leakage.

374 The rapid adoption of electric vehicles (EVs) serves as a prime example of
375 the potential atmospheric impacts of the zero-emission technological pathway
376 in the energy transition. Shifting to EVs powered by grid electricity from
377 renewable sources eliminates a primary source of CO₂ and especially NO_x
378 emissions in urban environments, but this transition introduces complex side
379 effects that require thorough investigation. The COVID-19 lockdowns provide a
380 revealing natural experiment analogous in many ways to the EVs transition, as
381 transportation emissions via internal combustion engine vehicles was
382 drastically reduced during this time. This emission reduction revealed the
383 nonlinear behavior and critical importance of AOC in secondary pollution

384 formation⁷². Global observations showed that although NO_x reductions
385 improved air quality in some regions⁷³, China experienced secondary pollution
386 bursts (O₃, particulate nitrate, and organics)⁷⁴⁻⁷⁵ and global CH₄ loss rates
387 declined undesirably⁴. These divergent, region-specific outcomes demonstrate
388 that the impacts of fossil fuels phase-out depend strongly on local chemical
389 regimes, shaped by the interplay of anthropogenic and biogenic emissions with
390 meteorological conditions. Notably, the air quality benefits are localized, but the
391 potential increases in CH₄ levels may exacerbate global climate impacts. This
392 disparity creates disproportionate burdens for developing countries,
393 underscoring a critical equity dilemma in climate mitigation policy. The EVs
394 transition thus serves as a critical warning, highlighting the imperative to
395 strategically manage AOC in order to navigate these inequities and complex
396 trade-offs.

397 Given the anticipated near-term persistence of CH₄ and reactive carbon
398 emissions, maintaining AOC will necessitate the strategic deployment of NO_x
399 emissions, despite their inherent trade-off with local air quality. This approach
400 is grounded in the spatial interdependence of the oxidation system: relocating
401 NO_x-emitting industries to tropical regions, which are characterized by high
402 oxidation capacity and function under NO_x-limited chemical regimes, could
403 enhance the OH levels responsible for global CH₄ removal, while reducing
404 ground-level O₃ and NO_x in populated areas⁷⁶. This offers a promising pathway
405 to co-managing air quality and climate mitigation. However, implementing such
406 geoengineering strategies is not a direct decision but a complex prospect
407 fraught with challenges. It first demands comprehensive evaluation across
408 three critical dimensions: (1) the ethical assessment of pollution burden
409 redistribution and its socioeconomic consequences, (2) a rigorous cost-benefit
410 analysis comparing AOC gains against local environmental and health costs,

411 and (3) the establishment of equitable compensation frameworks, potentially
412 integrated with carbon market mechanisms, to address regional disparities in
413 environmental impacts. Furthermore, even if deemed ethically and
414 economically viable, realizing this potential depends critically on the availability
415 of accurate numerical models capable of simulating the complex interactions
416 among meteorology, climate, and atmospheric chemistry in response to
417 anthropogenic emission changes⁵⁵. At present, the utility of Earth system
418 models for this task is hindered by considerable uncertainties, including
419 inaccuracies in emission inventories, oversimplified chemical mechanisms, and
420 insufficient coupling of key climate-chemistry feedbacks. Therefore, advancing
421 the predictive capability of these models is an essential prerequisite to
422 translating the concept of emission redistribution into credible, policy-relevant
423 strategies.

424 Hydrogen, as a clean energy carrier and carbon-neutral fuel, represents a
425 promising alternative pathway toward carbon neutrality, especially as
426 electrification generates surplus electricity for its production via electrolysis.
427 However, the large-scale deployment of H₂-based technologies, whether in fuel
428 cells or through combustion of H₂ or ammonia, introduces substantial
429 atmospheric risks that extend well beyond engineering and economic
430 constraints. The primary common risk is fugitive emission of H₂ and its
431 precursor, CH₄, across the supply chain. For instance, the 'blue hydrogen'
432 process, which utilizes CH₄ as feedstock to produce H₂ with CO₂ byproducts,
433 offers one potential pathway to meet global energy needs. Yet even with
434 perfect CO₂ capture, this approach remains prone to fugitive emissions of H₂
435 and CH₄ during transport and use, which could increase atmospheric CH₄
436 levels, thereby offsetting potential climate benefits^{17, 77}. Additionally, H₂
437 combustion produces water vapor that may influence climate systems from

438 local to global scales⁷⁸, and could potentially impact stratospheric chemistry⁷⁹.
439 Furthermore, the use of ammonia (NH₃) as a potential H₂ carrier and fuel, may
440 alter particulate acidity and exacerbate urban air pollution⁸⁰.

441 These emerging risks necessitate a full life-cycle environmental impact
442 assessment of H₂ prior to large-scale deployment⁸¹, particularly regarding the
443 response of atmospheric self-cleansing capacity to shifting emission patterns,
444 a relationship clearly demonstrated through historical OH records that reveal
445 how energy system transitions have fundamentally reshaped AOC.
446 Consequently, climate governance must undergo a fundamental paradigm shift
447 by elevating AOC stabilization to the same strategic priority as CO₂ mitigation
448 within policy frameworks. This is essential to avoid trading near-term gains for
449 long-term crises, such as compromised AOC, accelerated CH₄-driven warming,
450 and the inequitable pollution redistribution. This requires policies that integrate
451 chemical feedback mechanisms, informed by advanced atmospheric research
452 and historical evidence, to maintain Earth's self-cleansing capacity while
453 achieving emission targets.

454 **Advancing Next-Generation AOC Model Development**

455 **(a) Improving OH Chemistry in VOC-Rich Environments**

456 Current atmospheric chemistry models systematically underestimate AOC
457 in environments dominated by biogenic VOCs (BVOCs) and OVOCs, particularly
458 under low-NO_x conditions^{45,65,82}. This persistent model bias, evidenced by
459 consistent discrepancies between measured and simulated OH radical
460 concentrations^{16, 83-84}, points to critical gaps in our mechanistic understanding
461 of VOCs oxidation pathways²⁶. Key uncertainties involve the autoxidation
462 mechanisms of BVOC- and OVOC-derived RO₂ radicals, their
463 temperature-dependent H-shift tunneling kinetics, and the contribution of
464 unimolecular RO₂ reactions to OH recycling^{26, 85-86}. To address these gaps,

465 integrated laboratory, theoretical, and field studies are required to quantify the
466 rates and products of RO₂ isomerization and fragmentation reactions under
467 atmospherically relevant conditions. Incorporating these refined mechanisms
468 into next-generation chemical models is essential for accurate projection of OH
469 radical concentrations and AOC. This advancement is particularly urgent given
470 ongoing policy-driven emission changes, such as afforestation increasing
471 BVOC emissions and decarbonization reducing anthropogenic NO_x emissions,
472 and will provide a more robust scientific foundation for climate and air quality
473 policymaking.

474 **(b) Enhancing Climate-Chemistry Feedback in AOC Projections**

475 **Biogeochemical feedbacks:** Accurate projection of AOC under climate
476 change necessitates an integrated understanding of biogeochemical
477 feedbacks coupled with dynamic emission processes. Current models exhibit
478 substantial uncertainties, particularly in representing climate-sensitive
479 emissions and multi-scale chemical interactions. Addressing these gaps
480 demands a systematic effort to enhance the mechanistic representation of key
481 processes and to develop observationally constrained, predictive frameworks.
482 A primary challenge lies in quantifying climate-driven emissions of reactive
483 species. Rising temperatures amplify releases of VOCs from both
484 anthropogenic volatile chemical products (VCPs) and BVOCs. Concurrently,
485 natural methane emissions from wetlands and NO_x from soils and lightning are
486 perturbed by warming, while increasing wildfire activity contributes substantial
487 reactive gases and aerosols⁸⁷⁻⁹⁰. To reduce uncertainties in these fluxes, future
488 work should prioritize the development of process-based emission modules
489 responsive to climate forcing, supported by improved mechanistic
490 parameterizations and multi-platform observational constraints. Advanced
491 monitoring technologies, such as remote sensing, eddy covariance systems,

492 and chamber-based field measurements coupled with next-generation Earth
493 system models, will be critical to capture temperature-dependent changes in
494 AOC and to better project chemistry-climate feedbacks.

495 **Tropospheric halogen chemistry:** These complex interactions are further
496 compounded by significant uncertainties in halogen chemistry⁶⁴⁻⁶⁶, particularly
497 within the MBL, where persistent knowledge gaps limit our ability to accurately
498 quantify oxidative processes. Major challenges include insufficient kinetic data
499 for critical reactions (e.g. $\text{IO} + \text{CH}_3\text{O}_2$), sparse measurements of reactive halogen
500 species (RHS) such as IO and BrO that are essential for resolving their
501 spatiotemporal distributions, and poorly constrained emission estimates that
502 are likely to be intensified under climate change^{66, 91}. An especially pressing
503 priority is to refine the understanding of bromine (Br) in governing the
504 atmospheric lifetime of mercury (Hg), which currently shows high variability (4
505 to 40 days) due to uncertainties in Br sources. Although Br has traditionally
506 been ascribed to marine emissions, recent observations of elevated BrCl over
507 the NCP in China suggest the presence of additional, poorly quantified
508 terrestrial or anthropogenic sources⁶¹. Moreover, the activation pathways of
509 RHS, primarily mediated by NO_x , introduce further complexity, as future
510 reductions in NO_x emissions may fundamentally reshape these mechanisms in
511 ways not yet captured by models. Addressing these gaps demands a targeted
512 research strategy aimed at enhancing the identification of RHS source and
513 refining their representation in model. Critical steps comprise expanding field
514 measurements to better constrain spatiotemporal RHS variability, conducting
515 laboratory studies to resolve kinetic parameters, and integrating refined
516 halogen emission and chemistry modules into climate-chemistry models. Such
517 advancements are essential for reducing uncertainties in projections of Hg
518 cycling and enhancing the accuracy of halogen-mediated climate feedbacks.

519 **Interactions with troposphere-stratosphere:** Furthermore, evolving
520 emission patterns due to intensified industrial pollution controls are elevating
521 the relative importance of agricultural activities in atmospheric chemical
522 processes. The increased use of fertilizer and expansion of agricultural activity
523 are projected to enhance soil N₂O emissions, which may indirectly modulate
524 atmospheric CH₄ levels via complex stratosphere-troposphere interactions^{19,92}.
525 Stratospheric processes introduce additional complexity, with model
526 ensembles suggesting that stratospheric ozone accounts for approximately
527 25% of surface ozone concentrations, although inter-model variability exceeds
528 a factor of two⁹³. Furthermore, emerging evidence indicates that stratospheric
529 air intrusions can affect climate regimes by triggering large-scale new particle
530 formation events⁹⁴, revealing previously underappreciated
531 troposphere-stratosphere interactions that require systematic investigation
532 under future climate scenarios. Efforts to constrain these linkages must
533 integrate advanced observational networks with next-generation modelling
534 frameworks. Critical pathways forward involve improving the mechanistic
535 representation of agricultural N₂O and CH₄ coupling within Earth system
536 models, achieving higher vertical resolution to quantify
537 stratosphere-troposphere exchange processes, and deploying targeted field
538 campaigns to validate the impact of stratospheric intrusions on particle
539 formation and radiative forcing.

540 **(c) Coupling Methane and Chemistry in Earth System Models**

541 Current Earth system models predominantly rely on prescribed CH₄
542 concentrations rather than prognostic, emissions-based approaches. While
543 emerging model frameworks are beginning to incorporate interactive methane
544 cycling⁴⁷⁻⁴⁹, many widely used models still fail to capture the nonlinear coupling
545 between CH₄ emissions and atmospheric concentrations, neglecting critical

546 chemical feedbacks, particularly those involving radical chemistry. The
547 prescribed-concentration approach implicitly parameterizes OH levels using
548 simplified scaling factors for changes in OH precursors^{18,95}, introducing a
549 fundamental inconsistency in the representation of atmospheric oxidation
550 capacity. Significant uncertainties in CH₄ chemical loss rates, driven largely by
551 poor constraints on global OH concentrations, further impede the adoption of
552 emission-based approaches and amplify uncertainties in climate projections.

553 To advance Earth system modeling towards robust, emission-driven CH₄
554 simulations, a concerted effort is needed to reduce key mechanistic
555 uncertainties and develop advanced model configurations with fully interactive
556 CH₄ chemistry. A critical priority is to significantly reduce uncertainties in
557 atmospheric chemical sink processes, particularly the representation of OH
558 chemistry. This requires refining the spatiotemporal variability of OH
559 concentrations within models by improving the mechanistic understanding of
560 radical chemistry and the representation of key drivers, such as photolysis
561 rates, NO_x emissions, and VOC interactions. Enhanced coupling between
562 tropospheric chemistry and climate dynamics is also essential to capture
563 feedback mechanisms that modulate CH₄ lifetime under evolving scenarios.
564 Concurrently, process-based representations of methane sources, especially
565 climate-sensitive wetlands, thawing permafrost, and inland waters, require
566 improved mechanistic modelling of their hydrological, ecological, and
567 biogeochemical interactions. These modelling efforts must be strongly
568 supported and constrained by multi-platform observations that integrate
569 top-down remote sensing with bottom-up field measurements, enabling
570 improved emissions quantification and model validation through advanced
571 data assimilation. Ultimately, integrating these components into coupled
572 emission-chemistry modules that dynamically link anthropogenic and natural

573 sources with atmospheric oxidation processes will be crucial. Such
574 advancements will support a robust transition from concentration-driven to
575 emission-driven CH₄ representation, enabling more reliable projections of AOC
576 and better-informed evaluation of climate-air quality policy interactions.

577 **Global AOC Monitoring and Science-Based Policy**

578 The transition to low-carbon energy systems introduces complex
579 atmospheric trade-offs, underscoring the need to systematically monitor AOC
580 as a critical metric of Earth's atmospheric resilience. A robust global AOC
581 observation network would provide the essential data required to evaluate OH
582 concentrations, which govern the atmospheric self-cleansing capacity and the
583 lifetime of CH₄, as well as total OH reactivity that serves as a key proxy for
584 radical loss processes in atmospheric models. As outlined in Box 2, such an
585 integrated monitoring system would deliver quantitative, policy-relevant metrics
586 across spatial and temporal scales, bridging fundamental science and
587 decision-making.

588 Implementation this network requires coordinated advances across
589 multiple measurement technologies (Box 2). Existing ground-based
590 atmospheric supersites require upgrades with next-generation instrumentation
591 capable of simultaneous radical measurements and reactivity quantification.
592 The high costs of these technologies must be reduced through innovation in
593 laser spectroscopy and sensor miniaturization to enhance accessible.
594 Concurrently, novel satellite remote sensing methodologies must be developed
595 to achieve global mapping of OH distributions, extending coverage beyond
596 ground-based limitations⁹⁶. These parallel developments require sustained
597 international funding to establish standardized measurement protocols, ensure
598 cross-platform data compatibility, and maintain the long-term monitoring
599 necessary for detecting critical climate-chemistry feedback mechanisms.

600 The proposed AOC monitoring network offers equally significant scientific
601 and policy applications. By characterizing spatiotemporal patterns in AOC, it
602 would enable optimization of emission reduction strategies. For instance,
603 guiding industrial siting decisions that balance local air quality goals with
604 global atmospheric cleansing needs. The network's data products would
605 provide empirical benchmarks for assessing compliance with international
606 climate agreements like the Global Methane Pledge and Paris Agreement.
607 Furthermore, integration of AOC metrics into Earth system models would help
608 resolve current uncertainties in CH₄-OH feedback mechanisms that currently
609 constrain climate projections.

610 To operationalize this framework, we propose establishing an International
611 AOC Science Alliance that brings together atmospheric chemists, remote
612 sensing experts, and policy specialists. This consortium would oversee three
613 primary functions: (1) harmonization of measurement standards and quality
614 assurance across observational platforms; (2) development of open-access
615 data repositories featuring real-time analytics capabilities; and (3) translation of
616 scientific observations into actionable policy guidance for clean energy
617 transitions. Through such a coordinated global effort, it becomes feasible to
618 navigate the complex atmospheric impacts of decarbonization while preserving
619 the Earth's self-cleansing capacity during this critical transition.

620 **GOVERNING AOC FOR CLIMATE AND AIR QUALITY**
621 **CO-BENEFITS**

622 The transition toward carbon neutrality confronts a critical atmospheric
623 governance challenge: sustaining Earth's self-cleansing capacity while
624 simultaneously improving regional air quality and meeting global climate
625 objectives. Policymakers urgently need predictive, systemic tools capable of

626 quantifying the trade-offs and co-benefits between air quality management and
627 climate mitigation. However, a significant gap persists between current
628 atmospheric science capabilities and policy requirements. Existing climate
629 governance frameworks, including the Paris Agreement and Global Methane
630 Pledge, often lack mechanistic links to atmospheric chemistry, leaving
631 regulators without actionable insights into how emission changes impact
632 oxidative capacity, pollutant lifetimes, or secondary formation. To bridge this
633 gap, we propose an innovative AOC framework that translates complex
634 chemical processes into policy-operational metrics. This approach moves
635 beyond reactive regulation by embedding atmospheric feedbacks directly into
636 policy design, enabling proactive and integrated decision-making. We call for
637 the adoption of dynamic, chemistry-informed governance tools that align
638 emission pathways with AOC stability, ensuring that climate strategies do not
639 inadvertently compromise atmospheric resilience. Furthermore, we urge
640 enhanced collaboration between scientific and policy communities to
641 co-develop scalable, regionally tailored approaches that maintain oxidation
642 capacity throughout deep decarbonization. Looking forward, AOC must be
643 elevated from a passive chemical metric to a central governance pillar,
644 enabling smarter and more adaptive climate policy grounded in the realities of
645 atmospheric science.

646 **Acknowledgements:**

647 This work was supported by the National Natural Science Foundation of China
648 (grant 22325601, 42475110, and 22406003), the National Key R&D Program of
649 MoST China (2023YFC3706100, 2024YFC3713601, 2024YFC3712902, and
650 2023YFC3710900).

651 **Author contributions:**

652 Z.F.T. and X.F.M. designed and performed the study, and drafted and revised

653 the manuscript. K.D.L. and Y.H.Z. supervised the project and reviewed and
654 revised the manuscript. X.L., Q.D.Z., and F.R. created the figures and provided
655 analytical comments. A.N., H.F., A.W., L.W., D.H., S.B., and X.Z. contributed to
656 data interpretation, manuscript discussion, and critical revision.

657 **Declaration of interests:**

658 The authors declare no competing interests.

659 **References:**

- 660 1. Prinn, R.G. (2003). The Cleansing Capacity of the Atmosphere.
661 Annu. Rev. Environ. Resour. 28, 29-57.
- 662 2. Heald, C.L., Kroll, J.H. (2021). A radical shift in air pollution. Science.
663 374, 688-689.
- 664 3. Lu, K., Guo, S., Tan, Z., Wang, H., Shang, D., Liu, Y., Li, X., Wu, Z., Hu, M.,
665 Zhang, Y. (2019). Exploring atmospheric free-radical chemistry in China: the
666 self-cleansing capacity and the formation of secondary air pollution. National
667 Science Review. 6, 579-594.
- 668 4. Peng, S., Lin, X., Thompson, R.L., Xi, Y., Liu, G., Hauglustaine, D., Lan, X.,
669 Poulter, B., Ramonet, M., Saunois, M., et al. (2022). Wetland emission and
670 atmospheric sink changes explain methane growth in 2020. Nature. 612,
671 477-482.
- 672 5. Li, K., Jacob, D.J., Liao, H., Shen, L., Zhang, Q., Bates, K.H. (2019).
673 Anthropogenic drivers of 2013-2017 trends in summer surface ozone in China.
674 Proc Natl Acad Sci USA. 116, 422-427.
- 675 6. Huang, X., Ding, A., Gao, J., Zheng, B., Zhou, D., Qi, X., Tang, R., Wang, J.,
676 Ren, C., Nie, W., et al. (2020). Enhanced secondary pollution offset reduction of
677 primary emissions during COVID-19 lockdown in China. National Science
678 Review.
- 679 7. Yan, C., Tham, Y.J., Nie, W., Xia, M., Wang, H., Guo, Y., Ma, W., Zhan, J.,
680 Hua, C., Li, Y., et al. (2023). Increasing contribution of nighttime nitrogen
681 chemistry to wintertime haze formation in Beijing observed during COVID-19
682 lockdowns. Nature Geoscience. 16, 975-981.
- 683 8. Laughner, J.L., Neu, J.L., Schimel, D., Wennberg, P.O., Barsanti, K.,
684 Bowman, K.W., Chatterjee, A., Croes, B.E., Fitzmaurice, H.L., Henze, D.K., et al.
685 (2021). Societal shifts due to COVID-19 reveal large-scale complexities and
686 feedbacks between atmospheric chemistry and climate change. Proc. Natl.

687 Acad. Sci. U.S.A. 118, e2109481118.

688 9. Fu, B., Li, J., Jiang, Y., Chen, Z., Li, B. (2024). Clean air policy makes
689 methane harder to control due to longer lifetime. One Earth. 7, 1266-1274.

690 10. Prather, M.J. (1996). Time scales in atmospheric chemistry:
691 Theory, GWPs for CH₄ and CO, and runaway growth. Geophys. Res. Lett. 23,
692 2597-2600.

693 11. Tan, Z., Lu, K., Jiang, M., Su, R., Wang, H., Lou, S., Fu, Q., Zhai, C.,
694 Tan, Q., Yue, D., et al. (2019). Daytime atmospheric oxidation capacity in four
695 Chinese megacities during the photochemically polluted season: a case study
696 based on box model simulation. Atmospheric Chemistry and Physics. 19,
697 3493-3513.

698 12. Lyu, X., Li, K., Guo, H., Morawska, L., Zhou, B.N., Zeren, Y., Jiang, F.,
699 Chen, C.H., Goldstein, A.H., Xu, X.B., et al. (2023). A synergistic ozone-climate
700 control to address emerging ozone pollution challenges. One Earth. 6, 964-977.

701 13. Tan, Z.F., Lu, K.D., Ma, X.F., Chen, S.Y., He, L.Y., Huang, X.F., Li, X.,
702 Lin, X.Y., Tang, M.X., Yu, D., et al. (2022). Multiple Impacts of Aerosols on O₃
703 Production Are Largely Compensated: A Case Study Shenzhen, China.
704 Environmental Science&Technology.

705 14. Tan, Z.F., Hofzumahaus, A., Lu, K.D., Brown, S.S., Holland, F., Huey,
706 L.G., Kiendler-Scharr, A., Li, X., Liu, X.X., Ma, N., et al. (2020). No Evidence for a
707 Significant Impact of Heterogeneous Chemistry on Radical Concentrations in
708 the North China Plain in Summer 2014. Environmental Science&Technology. 54,
709 5973-5979.

710 15. Levy, H. (1971). Normal atmosphere: large radical and
711 formaldehyde concentrations predicted. Science. 173, 141-&.

712 16. Lu, K.D., Rohrer, F., Holland, F., Fuchs, H., Bohn, B., Brauers, T.,
713 Chang, C.C., Haseler, R., Hu, M., Kita, K., et al. (2012). Observation and
714 modelling of OH and HO₂ concentrations in the Pearl River Delta 2006: a
715 missing OH source in a VOC rich atmosphere. Atmos. Chem. Phys. 12,
716 1541-1569.

717 17. Schultz, M.G., Diehl, T., Brasseur, G.P., Zittel, W. (2003). Air
718 Pollution and Climate-Forcing Impacts of a Global Hydrogen Economy.
719 Science. 302, 624-627.

720 18. Liu, M., Song, Y., Matsui, H., Shang, F., Kang, L., Cai, X., Zhang, H.,
721 Zhu, T. (2024). Enhanced atmospheric oxidation toward carbon neutrality
722 reduces methane's climate forcing. Nature Communications. 15, 3148.

723 19. Prather, M.J., Hsu, J. (2010). Coupling of Nitrous Oxide and

724 Methane by Global Atmospheric Chemistry. *Science*. 330, 952-954.

725 20. Tan, Z.F., Lu, K.D., Jiang, M.Q., Su, R., Wang, H.L., Lou, S.R., Fu,
726 Q.Y., Zhai, C.Z., Tan, Q.W., Yue, D.L., et al. (2019). Daytime atmospheric
727 oxidation capacity in four Chinese megacities during the photochemically
728 polluted season: a case study based on box model simulation. *Atmospheric
729 Chemistry and Physics*. 19, 3493-3513.

730 21. Tan, Z., Lu, K., Jiang, M., Su, R., Dong, H., Zeng, L., Xie, S., Tan, Q.,
731 Zhang, Y. (2018). Exploring ozone pollution in Chengdu, southwestern China: A
732 case study from radical chemistry to O₃-VOC-NO_x sensitivity. *Science of the
733 Total Environment*. 636, 775-786.

734 22. Zhao, Y., Zheng, B., Saunois, M., Ciais, P., Hegglin, M.I., Lu, S., Li, Y.,
735 Bousquet, P. (2025). Air pollution modulates trends and variability of the global
736 methane budget. *Nature*. 642, 369-375.

737 23. Tarasick, D., Galbally, I.E., Cooper, O.R., Schultz, M.G., Ancellet, G.,
738 Leblanc, T., Wallington, T.J., Ziemke, J., Liu, X., Steinbacher, M., et al. (2019).
739 Tropospheric Ozone Assessment Report: Tropospheric ozone from 1877 to
740 2016, observed levels, trends and uncertainties. *Elementa: Science of the
741 Anthropocene*. 7.

742 24. Stevenson, D.S., Zhao, A., Naik, V., O'Connor, F.M., Tilmes, S., Zeng,
743 G., Murray, L.T., Collins, W.J., Griffiths, P.T., Shim, S., et al. (2020). Trends in
744 global tropospheric hydroxyl radical and methane lifetime since 1850 from
745 AerChemMIP. *Atmos. Chem. Phys.* 20, 12905-12920.

746 25. Murray, L.T., Fiore, A.M., Shindell, D.T., Naik, V., Horowitz, L.W.
747 (2021). Large uncertainties in global hydroxyl projections tied to fate of reactive
748 nitrogen and carbon. *Proc Natl Acad Sci U S A*. 118, e2115204118.

749 26. Rohrer, F., Lu, K., Hofzumahaus, A., Bohn, B., Brauers, T., Chang,
750 C.-C., Fuchs, H., Haseler, R., Holland, F., Hu, M., et al. (2014). Maximum
751 efficiency in the hydroxyl-radical-based self-cleansing of the troposphere. *Nat.
752 Geosci.* 7, 559-563.

753 27. Tan, Z., Lu, K., Ma, X., Chen, S., He, L., Huang, X., Li, X., Lin, X., Tang,
754 M., Yu, D., et al. (2022). Multiple Impacts of Aerosols on O₃ Production Are
755 Largely Compensated: A Case Study Shenzhen, China. *Environ. Sci. Technol.* 56,
756 17569-17580.

757 28. Whalley, L.K., Furneaux, K.L., Goddard, A., Lee, J.D., Mahajan, A.,
758 Oetjen, H., Read, K.A., Kaaden, N., Carpenter, L.J., Lewis, A.C., et al. (2010). The
759 chemistry of OH and HO₂ radicals in the boundary layer over the tropical
760 Atlantic Ocean. *Atmos. Chem. Phys.* 10, 1555-1576.

761 29. Ehhalt, D.H., Rohrer, F., Wahner, A. TROPOSPHERIC CHEMISTRY

762 AND COMPOSITION | Oxidizing Capacity. In: North GR, Pyle J, Zhang F, editors.
763 Encyclopedia of Atmospheric Sciences (Second Edition). Oxford: Academic
764 Press; 2015. p. 243-250.

765 30. Turner, A.J., Frankenberg, C., Kort, E.A. (2019). Interpreting
766 contemporary trends in atmospheric methane. Proc. Natl. Acad. Sci. U.S.A. 116,
767 2805.

768 31. Turner, A.J., Frankenberg, C., Wennberg, P.O., Jacob, D.J. (2017).
769 Ambiguity in the causes for decadal trends in atmospheric methane and
770 hydroxyl. Proc. Natl. Acad. Sci. U.S.A. 114, 5367.

771 32. Rigby, M., Montzka, S.A., Prinn, R.G., White, J.W.C., Young, D., O'
772 Doherty, S., Lunt, M.F., Ganesan, A.L., Manning, A.J., Simmonds, P.G., et al.
773 (2017). Role of atmospheric oxidation in recent methane growth. Proc. Natl.
774 Acad. Sci. U.S.A. 114, 5373.

775 33. Fiore, A.M., Hancock, S.E., Lamarque, J.-F., Correa, G.P., Chang,
776 K.-L., Ru, M., Cooper, O., Gaudel, A., Polvani, L.M., Sauvage, B., et al. (2022).
777 Understanding recent tropospheric ozone trends in the context of large internal
778 variability: a new perspective from chemistry-climate model ensembles.
779 Environ. Sci. Technol. 1, 025008.

780 34. Turner, A.J., Frankenberg, C., Kort, E.A. (2019). Interpreting
781 contemporary trends in atmospheric methane. Proceedings of the National
782 Academy of Sciences. 116, 2805.

783 35. Feng, L., Palmer, P.I., Zhu, S., Parker, R.J., Liu, Y. (2022). Tropical
784 methane emissions explain large fraction of recent changes in global
785 atmospheric methane growth rate. Nature Communications. 13, 1378.

786 36. Feng, L., Palmer, P.I., Parker, R.J., Lunt, M.F., Bösch, H. (2023).
787 Methane emissions are predominantly responsible for record-breaking
788 atmospheric methane growth rates in 2020 and 2021. Atmos. Chem. Phys. 23,
789 4863-4880.

790 37. Wang, Y., Jacob, D.J. (1998). Anthropogenic forcing on
791 tropospheric ozone and OH since preindustrial times. J. Geophys. Res. Atmos.
792 103, 31123-31135.

793 38. Patra, P.K., Krol, M.C., Montzka, S.A., Arnold, T., Atlas, E.L., Lintner,
794 B.R., Stephens, B.B., Xiang, B., Elkins, J.W., Fraser, P.J., et al. (2014).
795 Observational evidence for interhemispheric hydroxyl-radical parity. Nature.
796 513, 219-223.

797 39. Zhu, Q., Laughner, J.L., Cohen, R.C. (2022). Estimate of OH trends
798 over one decade in North American cities. Proc Natl Acad Sci U S A. 119,
799 e2117399119.

800 40. Wang, Y., Zhao, Y., Liu, Y., Jiang, Y., Zheng, B., Xing, J., Liu, Y.,
801 Wang, S., Nielsen, C.P. (2023). Sustained emission reductions have restrained
802 the ozone pollution over China. *Nat. Geosci.*

803 41. An, Z., Huang, R.-J., Zhang, R., Tie, X., Li, G., Cao, J., Zhou, W., Shi,
804 Z., Han, Y., Gu, Z., et al. (2019). Severe haze in northern China: A synergy of
805 anthropogenic emissions and atmospheric processes. *Proc. Natl. Acad. Sci.*
806 U.S.A. 116, 8657-8666.

807 42. Zheng, B., Tong, D., Li, M., Liu, F., Hong, C., Geng, G., Li, H., Li, X.,
808 Peng, L., Qi, J., et al. (2018). Trends in China's anthropogenic emissions since
809 2010 as the consequence of clean air actions. *Atmos. Chem. Phys.* 18,
810 14095-14111.

811 43. Wang, W., Li, X., Cheng, Y., Parrish, D.D., Ni, R., Tan, Z., Liu, Y., Lu,
812 S., Wu, Y., Chen, S., et al. (2023). Ozone pollution mitigation strategy informed
813 by long-term trends of atmospheric oxidation capacity. *Nature Geoscience*.

814 44. Nussbaumer, C.M., Cohen, R.C. (2020). The Role of Temperature
815 and NO_x in Ozone Trends in the Los Angeles Basin. *Environmental*
816 *Science&Technology*. 54, 15652-15659.

817 45. Pfannerstill, E.Y., Arata, C., Zhu, Q., Schulze, B.C., Ward, R., Woods,
818 R., Harkins, C., Schwantes, R.H., Seinfeld, J.H., Bucholtz, A., et al. (2024).
819 Temperature-dependent emissions dominate aerosol and ozone formation in
820 Los Angeles. *Science*. 384, 1324-1329.

821 46. Laughner, J.L., Cohen, R.C. (2019). Direct observation of changing
822 NO_x lifetime in North American cities. *Science*. 366, 723-727.

823 47. Folberth, G.A., Staniaszek, Z., Archibald, A.T., Gedney, N., Griffiths,
824 P.T., Jones, C.D., O'Connor, F.M., Parker, R.J., Sellar, A.A., Wiltshire, A. (2022).
825 Description and Evaluation of an Emission-Driven and Fully Coupled Methane
826 Cycle in UKESM1. *Journal of Advances in Modeling Earth Systems*. 14,
827 e2021MS002982.

828 48. Ocko, I.B., Sun, T.Y., Shindell, D., Oppenheimer, M., Hristov, A.N.,
829 Pacala, S.W., Mauzerall, D.L., Xu, Y.Y., Hamburg, S.P. (2021). Acting rapidly to
830 deploy readily available methane mitigation measures by sector can
831 immediately slow global warming. *Environmental Research Letters*. 16.

832 49. Im, U., Tsigaridis, K., Bauer, S., Shindell, D., Olivié, D., Wilson, S.,
833 Sorensen, L.L., Langen, P., Eckhardt, S. (2025). Future CH₄ as modelled by a
834 fully coupled Earth system model: prescribed GHG concentrations vs.
835 interactive CH₄ sources and sinks. *Environmental Research-Climate*. 4.

836 50. Naus, S., Montzka, S.A., Patra, P.K., Krol, M.C. (2021). A
837 three-dimensional-model inversion of methyl chloroform to constrain the

838 atmospheric oxidative capacity. *Atmos. Chem. Phys.* 21, 4809-4824.

839 51. Griffiths, P.T., Murray, L.T., Zeng, G., Shin, Y.M., Abraham, N.L.,
840 Archibald, A.T., Deushi, M., Emmons, L.K., Galbally, I.E., Hassler, B., et al. (2021).
841 Tropospheric ozone in CMIP6 simulations. *Atmos. Chem. Phys.* 21, 4187-4218.

842 52. Murray, L.T., Logan, J.A., Jacob, D.J. (2013). Interannual variability
843 in tropical tropospheric ozone and OH: The role of lightning. *J. Geophys. Res.*
844 *Atmos.* 118, 11,468-11,480.

845 53. Brune, W.H., McFarland, P.J., Bruning, E., Waugh, S., MacGorman,
846 D., Miller, D.O., Jenkins, J.M., Ren, X., Mao, J., Peischl, J. (2021). Extreme
847 oxidant amounts produced by lightning in storm clouds. *Science.* eabg0492.

848 54. Pérez-Invernón, F.J., Gordillo-Vázquez, F.J., Huntrieser, H., Jöckel,
849 P. (2023). Variation of lightning-ignited wildfire patterns under climate change.
850 *Nat. Comm.* 14, 739.

851 55. Lelieveld, J., Gromov, S., Pozzer, A., Taraborrelli, D. (2016). Global
852 tropospheric hydroxyl distribution, budget and reactivity. *Atmos. Chem. Phys.*
853 16, 12477-12493.

854 56. Edwards, P.M., Brown, S.S., Roberts, J.M., Ahmadov, R., Banta,
855 R.M., deGouw, J.A., Dube, W.P., Field, R.A., Flynn, J.H., Gilman, J.B., et al. (2014).
856 High winter ozone pollution from carbonyl photolysis in an oil and gas basin.
857 *Nature.* 514, 351-354.

858 57. Schnell, R.C., Oltmans, S.J., Neely, R.R., Endres, M.S., Molenar, J.V.,
859 White, A.B. (2009). Rapid photochemical production of ozone at high
860 concentrations in a rural site during winter. *Nat. Geosci.* 2, 120-122.

861 58. Lu, K., Fuchs, H., Hofzumahaus, A., Tan, Z., Wang, H., Zhang, L.,
862 Schmitt, S.H., Rohrer, F., Bohn, B., Broch, S., et al. (2019). Fast Photochemistry in
863 Wintertime Haze: Consequences for Pollution Mitigation Strategies. *Environ.*
864 *Sci. Technol.* 53, 10676-10684.

865 59. Slater, E.J., Whalley, L.K., Woodward-Massey, R., Ye, C., Lee, J.D.,
866 Squires, F., Hopkins, J.R., Dunmore, R.E., Shaw, M., Hamilton, J.F., et al. (2020).
867 Elevated levels of OH observed in haze events during wintertime in central
868 Beijing. *Atmos. Chem. Phys.* 20, 14847-14871.

869 60. Li, K., Jacob, D.J., Liao, H., Qiu, Y., Shen, L., Zhai, S., Bates, K.H.,
870 Sulprizio, M.P., Song, S., Lu, X., et al. (2021). Ozone pollution in the North China
871 Plain spreading into the late-winter haze season. *Proc. Natl. Acad. Sci. U.S.A.*
872 118, e2015797118.

873 61. Peng, X., Wang, W., Xia, M., Chen, H., Ravishankara, A.R., Li, Q.,
874 Saiz-Lopez, A., Liu, P., Zhang, F., Zhang, C., et al. (2021). An unexpected large

875 continental source of reactive bromine and chlorine with significant impact on
876 wintertime air quality. *Natl. Sci. Rev.* 8.

877 62. Wang, Y., Fu, X., Wang, T., Ma, J., Gao, H., Wang, X., Pu, W. (2023).
878 Large Contribution of Nitrous Acid to Soil-Emitted Reactive Oxidized Nitrogen
879 and Its Effect on Air Quality. *Environ. Sci. Technol.* 57, 3516-3526.

880 63. Lu, X., Ye, X., Zhou, M., Zhao, Y., Weng, H., Kong, H., Li, K., Gao, M.,
881 Zheng, B., Lin, J., et al. (2021). The underappreciated role of agricultural soil
882 nitrogen oxide emissions in ozone pollution regulation in North China. *Nat.*
883 *Comm.* 12, 5021.

884 64. Womack, C.C., Chace, W.S., Wang, S., Baasandorj, M., Fibiger, D.L.,
885 Franchin, A., Goldberger, L., Harkins, C., Jo, D.S., Lee, B.H., et al. (2023).
886 Midlatitude Ozone Depletion and Air Quality Impacts from Industrial Halogen
887 Emissions in the Great Salt Lake Basin. *Environ. Sci. Technol.* 57, 1870-1881.

888 65. Thornton, J.A., Kercher, J.P., Riedel, T.P., Wagner, N.L., Cozic, J.,
889 Holloway, J.S., Dube, W.P., Wolfe, G.M., Quinn, P.K., Middlebrook, A.M., et al.
890 (2010). A large atomic chlorine source inferred from mid-continental reactive
891 nitrogen chemistry. *Nature.* 464, 271-274.

892 66. Saiz-Lopez, A., Fernandez, R.P., Li, Q., Cuevas, C.A., Fu, X.,
893 Kinnison, D.E., Tilmes, S., Mahajan, A.S., Gómez Martín, J.C., Iglesias-Suarez, F.,
894 et al. (2023). Natural short-lived halogens exert an indirect cooling effect on
895 climate. *Nature.* 618, 967-973.

896 67. Jiang, X. (2023). A conversation on air pollution in India. *Nat.*
897 *Comm.* 16, 937-938.

898 68. Zheng, G., Su, H., Wang, S., Andreae, M.O., Pöschl, U., Cheng, Y.
899 (2020). Multiphase buffer theory explains contrasts in atmospheric aerosol
900 acidity. *Science.* 369, 1374-1377.

901 69. Poschl, U., Shiraiwa, M. (2015). Multiphase Chemistry at the
902 Atmosphere-Biosphere Interface Influencing Climate and Public Health in the
903 Anthropocene. *Chem. Rev.* 115, 4440-4475.

904 70. Chua, G., Naik, V., Horowitz, L.W. (2023). Exploring the drivers of
905 tropospheric hydroxyl radical trends in the Geophysical Fluid Dynamics
906 Laboratory AM4.1 atmospheric chemistry-climate model. *Atmos. Chem. Phys.*
907 23, 4955-4975.

908 71. Rohrer, F., Berresheim, H. (2006). Strong correlation between
909 levels of tropospheric hydroxyl radicals and solar ultraviolet radiation. *Nature.*
910 442, 184-187.

911 72. Shi, Z., Song, C., Liu, B., Lu, G., Xu, J., Van Vu, T., Elliott, R.J.R., Li,

912 W., Bloss, W.J., Harrison, R.M. (2021). Abrupt but smaller than expected
913 changes in surface air quality attributable to COVID-19 lockdowns. *Science*
914 *Advances*. 7, eabd6696.

915 73. Venter, Z.S., Aunan, K., Chowdhury, S., Lelieveld, J. (2020).
916 COVID-19 lockdowns cause global air pollution declines. *Proceedings of the*
917 *National Academy of Sciences*. 117, 18984-18990.

918 74. Tan, Z., Feng, M., Liu, H., Luo, Y., Li, W., Song, D., Tan, Q., Ma, X., Lu,
919 K., Zhang, Y. (2024). Atmospheric Oxidation Capacity Elevated during 2020
920 Spring Lockdown in Chengdu, China: Lessons for Future Secondary Pollution
921 Control. *Environmental Science&Technology*.

922 75. Huang, X., Ding, A., Gao, J., Zheng, B., Zhou, D., Qi, X., Tang, R.,
923 Wang, J., Ren, C., Nie, W., et al. (2021). Enhanced secondary pollution offset
924 reduction of primary emissions during COVID-19 lockdown in China. *National*
925 *Science Review*. 8.

926 76. Fiore, A.M., Mickley, L.J., Zhu, Q., Baublitz, C.B. (2024). Climate
927 and Tropospheric Oxidizing Capacity. *Annual Review of Earth and Planetary*
928 *Sciences*. 52, null.

929 77. Bertagni, M.B., Pacala, S.W., Paulot, F., Porporato, A. (2022). Risk
930 of the hydrogen economy for atmospheric methane. *Nat. Comm.* 13, 7706.

931 78. Keith, D.W., Farrell, A.E. (2003). Rethinking Hydrogen Cars.
932 *Science*. 301, 315-316.

933 79. Tromp, T.K., Shia, R.-L., Allen, M., Eiler, J.M., Yung, Y.L. (2003).
934 Potential Environmental Impact of a Hydrogen Economy on the Stratosphere.
935 *Science*. 300, 1740-1742.

936 80. Liu, M., Huang, X., Song, Y., Tang, J., Cao, J., Zhang, X., Zhang, Q.,
937 Wang, S., Xu, T., Kang, L., et al. (2019). Ammonia emission control in China
938 would mitigate haze pollution and nitrogen deposition, but worsen acid rain.
939 *Proc. Natl. Acad. Sci. U.S.A.* 116, 7760-7765.

940 81. Pielke, R.A., Klein, R., Maricle, G., Chase, T. (2003). Hydrogen Cars
941 and Water Vapor. *Science*. 302, 1329-1329.

942 82. Qin, M., Murphy, B.N., Isaacs, K.K., McDonald, B.C., Lu, Q., McKeen,
943 S.A., Koval, L., Robinson, A.L., Efstathiou, C., Allen, C., et al. (2020). Criteria
944 pollutant impacts of volatile chemical products informed by near-field
945 modelling. *Nature Sustainability*.

946 83. Hofzumahaus, A., Rohrer, F., Lu, K., Bohn, B., Brauers, T., Chang,
947 C.C., Fuchs, H., Holland, F., Kita, K., Kondo, Y., et al. (2009). Amplified trace gas
948 removal in the troposphere. *Science*. 324, 1702-1704.

949 84. Yang, X., Wang, H., Lu, K., Ma, X., Tan, Z., Long, B., Chen, X., Li, C.,
950 Zhai, T., Li, Y., et al. (2024). Reactive aldehyde chemistry explains the missing
951 source of hydroxyl radicals. *Nature Communications*. 15, 1648.

952 85. Liu, F., Beames, J.M., Petit, A.S., McCoy, A.B., Lester, M.I. (2014).
953 Infrared-driven unimolecular reaction of CH₃CHOO Criegee intermediates to OH
954 radical products. *Science*. 345, 1596-1598.

955 86. Praske, E., Otkjær, R.V., Crounse, J.D., Hethcox, J.C., Stoltz, B.M.,
956 Kjaergaard, H.G., Wennberg, P.O. (2018). Atmospheric autoxidation is
957 increasingly important in urban and suburban North America. *Proceedings of
958 the National Academy of Sciences*. 115, 64-69.

959 87. Theys, N., Volkamer, R., Muller, J.F., Zarzana, K.J., Kille, N.,
960 Clarissoe, L., De Smedt, I., Lerot, C., Finkenzeller, H., Hendrick, F., et al. (2020).
961 Global nitrous acid emissions and levels of regional oxidants enhanced by
962 wildfires. *Nat. Geosci.* 13, 681-+.

963 88. Xu, L., Crounse, J.D., Vasquez, K.T., Allen, H., Wennberg, P.O.,
964 Bourgeois, I., Brown, S.S., Campuzano-Jost, P., Coggon, M.M., Crawford, J.H., et
965 al. (2021). Ozone chemistry in western U.S. wildfire plumes. *Sci. Adv.* 7,
966 eabl3648.

967 89. Huang, X., Ding, K., Liu, J.Y., Wang, Z.L., Tang, R., Xue, L., Wang,
968 H.K., Zhang, Q., Tan, Z.M., Fu, C.B., et al. (2023). Smoke-weather interaction
969 affects extreme wildfires in diverse coastal regions. *Science*. 379, 457-461.

970 90. Thornhill, G., Collins, W., Olivié, D., Skeie, R.B., Archibald, A., Bauer,
971 S., Checa-Garcia, R., Fiedler, S., Folberth, G., Gjermundsen, A., et al. (2021).
972 Climate-driven chemistry and aerosol feedbacks in CMIP6 Earth system
973 models. *Atmos. Chem. Phys.* 21, 1105-1126.

974 91. Tham, Y.J., Sarnela, N., Iyer, S., Li, Q., Angot, H., Quéléver, L.L.J.,
975 Beck, I., Laurila, T., Beck, L.J., Boyer, M., et al. (2023). Widespread detection of
976 chlorine oxyacids in the Arctic atmosphere. *Nature Communications*. 14, 1769.

977 92. Gong, C., Tian, H., Liao, H., Pan, N., Pan, S., Ito, A., Jain, A.K.,
978 Kou-Giesbrecht, S., Joos, F., Sun, Q., et al. (2024). Global net climate effects of
979 anthropogenic reactive nitrogen. *Nature*.

980 93. Li, Y., Xia, Y., Xie, F., Yan, Y. (2024). Influence of
981 stratosphere-troposphere exchange on long-term trends of surface ozone in
982 CMIP6. *Atmospheric Research*. 297, 107086.

983 94. Zhang, J., Gong, X., Crosbie, E., Diskin, G., Froyd, K., Hall, S., Kupc,
984 A., Moore, R., Peischl, J., Rollins, A., et al. (2024). Stratospheric air intrusions
985 promote global-scale new particle formation. *Science*. 385, 210-216.

986 95. Meinshausen, M., Raper, S.C.B., Wigley, T.M.L. (2011). Emulating
987 coupled atmosphere-ocean and carbon cycle models with a simpler model,
988 MAGICC6 – Part 1: Model description and calibration. *Atmos. Chem. Phys.* 11,
989 1417-1456.

990 96. Pimplott, M.A., Pope, R.J., Kerridge, B.J., Latter, B.G., Knappett, D.S.,
991 Heard, D.E., Ventress, L.J., Siddans, R., Feng, W., Chipperfield, M.P. (2022).
992 Investigating the global OH radical distribution using steady-state
993 approximations and satellite data. *Atmos. Chem. Phys.* 22, 10467-10488.

994 97. Lelieveld, J., Butler, T.M., Crowley, J.N., Dillon, T.J., Fischer, H.,
995 Ganzeveld, L., Harder, H., Lawrence, M.G., Martinez, M., Taraborrelli, D., et al.
996 (2008). Atmospheric oxidation capacity sustained by a tropical forest. *Nature*.
997 452, 737-740.

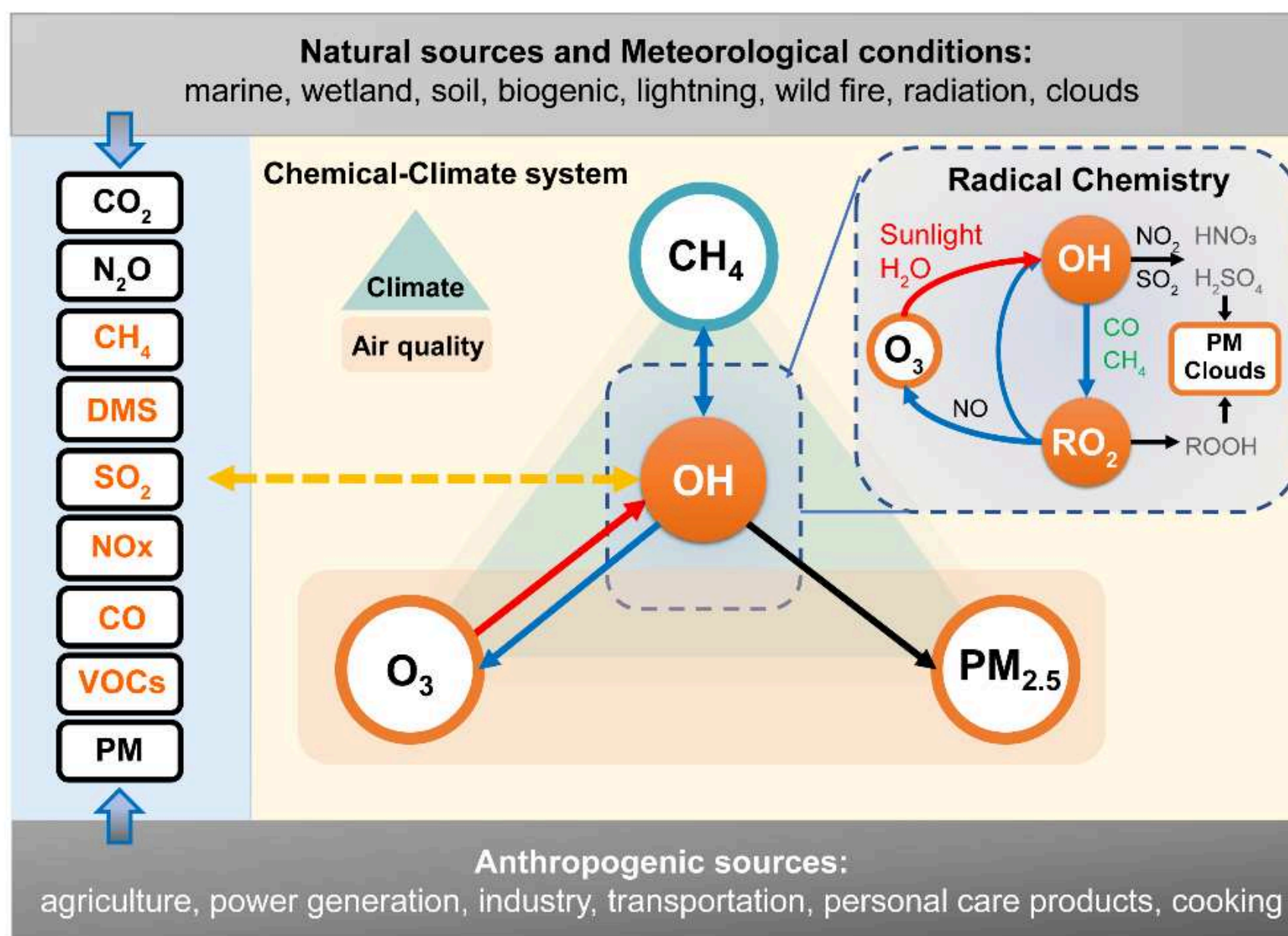
998 98. Lu, K.D., Hofzumahaus, A., Holland, F., Bohn, B., Brauers, T., Fuchs,
999 H., Hu, M., Haseler, R., Kita, K., Kondo, Y., et al. (2013). Missing OH source in a
1000 suburban environment near Beijing: observed and modelled OH and HO₂
1001 concentrations in summer 2006. *Atmos. Chem. Phys.* 13, 1057-1080.

1002 99. Tan, Z., Lu, K., Dong, H., Hu, M., Li, X., Liu, Y., Lu, S., Shao, M., Su, R.,
1003 Wang, H., et al. (2018). Explicit diagnosis of the local ozone production rate and
1004 the ozone-NO_x-VOC sensitivities. *Sci. Bull.* 63, 1067-1076.

1005 100. Stone, D., Whalley, L.K., Heard, D.E. (2012). Tropospheric OH and
1006 HO₂ radicals: field measurements and model comparisons. *Chemical Society
1007 Reviews*. 41, 6348-6404.

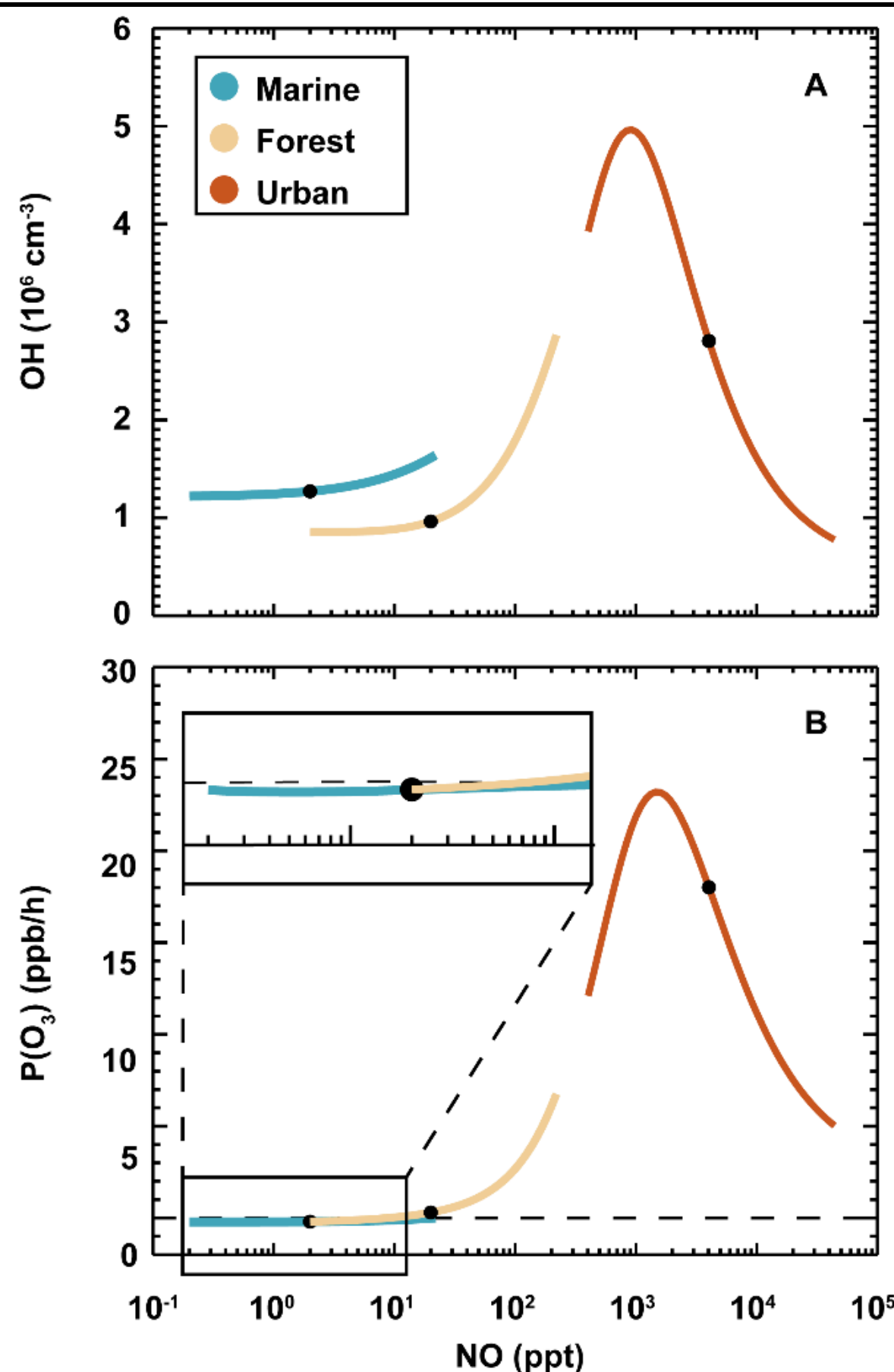
1008

1009

1010 **Figures and Tables:**

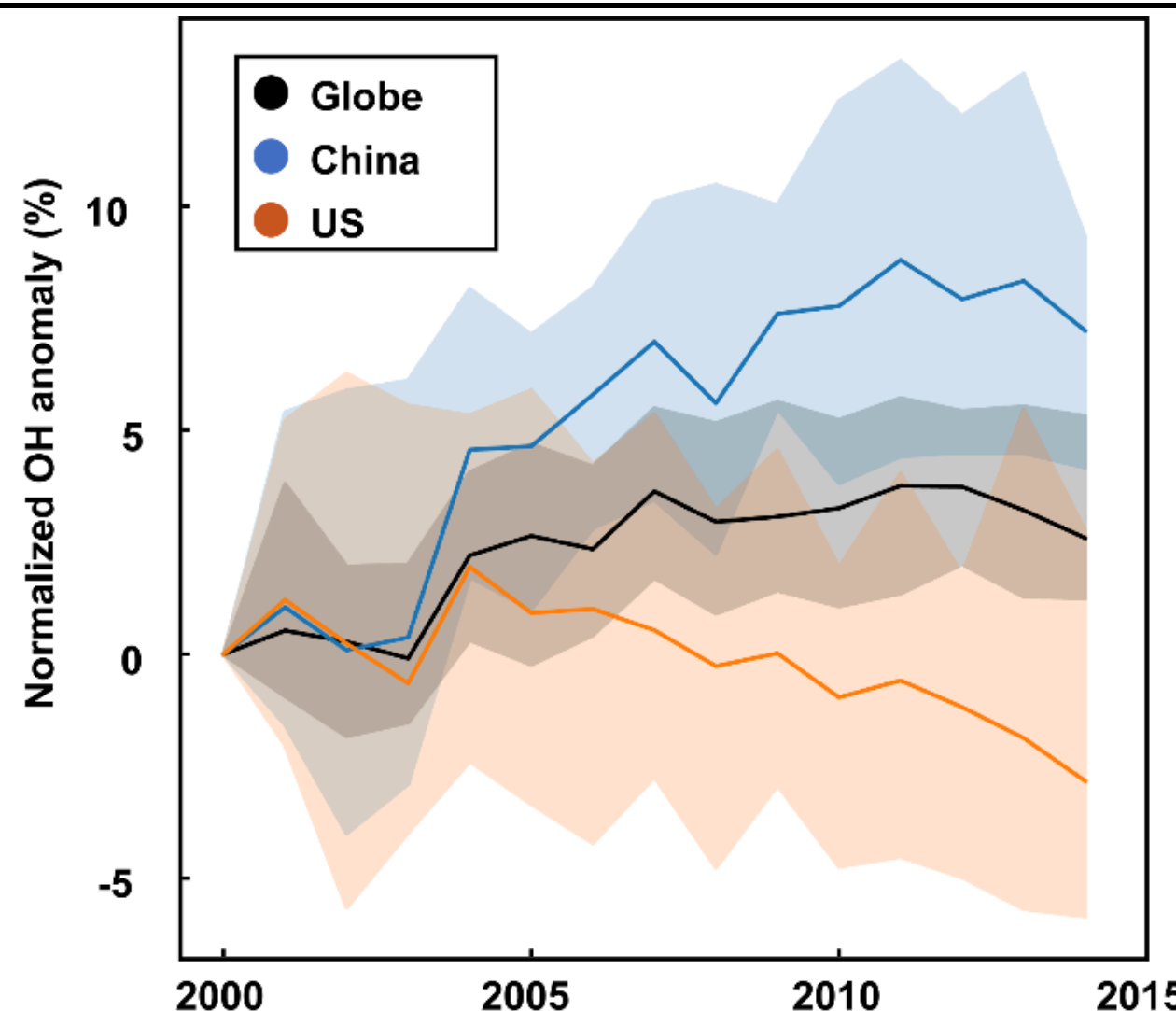
1011

1012 **Figure 1: Schematic representation of tropospheric chemistry-climate**
 1013 **interactions.** OH governs the atmospheric lifetime of CH₄, a potent greenhouse
 1014 gas, and drives the formation of secondary pollutants such as ozone and PM_{2.5},
 1015 which also act as significant climate forcers. It plays a critical role in linking air
 1016 pollution and climate forcing by mediating key atmospheric chemical
 1017 processes. Orange-highlighted species in the left panel represent reactive
 1018 gases from anthropogenic and biogenic sources that undergo OH-initiated
 1019 oxidation, while those marked in black denote emitted non-reactive greenhouse
 1020 gases and pollutants. Blue arrows indicate the oxidation pathways of reactive
 1021 carbon compounds (e.g., CH₄, CO, and VOCs), leading to the formation of
 1022 secondary pollutants including O₃ and PM_{2.5}. The red arrow denotes the
 1023 photolysis of O₃ to O(¹D), followed by reaction with water vapor, representing
 1024 the dominant global source of OH. The black arrow denotes the oxidation
 1025 processes involving NO_x, SO₂, and VOCs that contribute to the production of
 1026 secondary aerosols, such as nitrate, sulfate, and organic aerosols. The inset
 1027 presents a simplified scheme of global tropospheric photochemistry. CH₄
 1028 serves as a key representative of OH-oxidized gases (including CO, H₂, VOCs),
 1029 producing HO₂ and RO₂; RO₂ is a placeholder for peroxy radicals like HO₂ and
 1030 RO₂ which react with NO to form NO₂; ROOH represents peroxides (e.g., HOOH,
 1031 ROOH, and ROOR), which act as critical precursors to particulate matter (PM)
 1032 and influence cloud formation, thereby affecting climate.



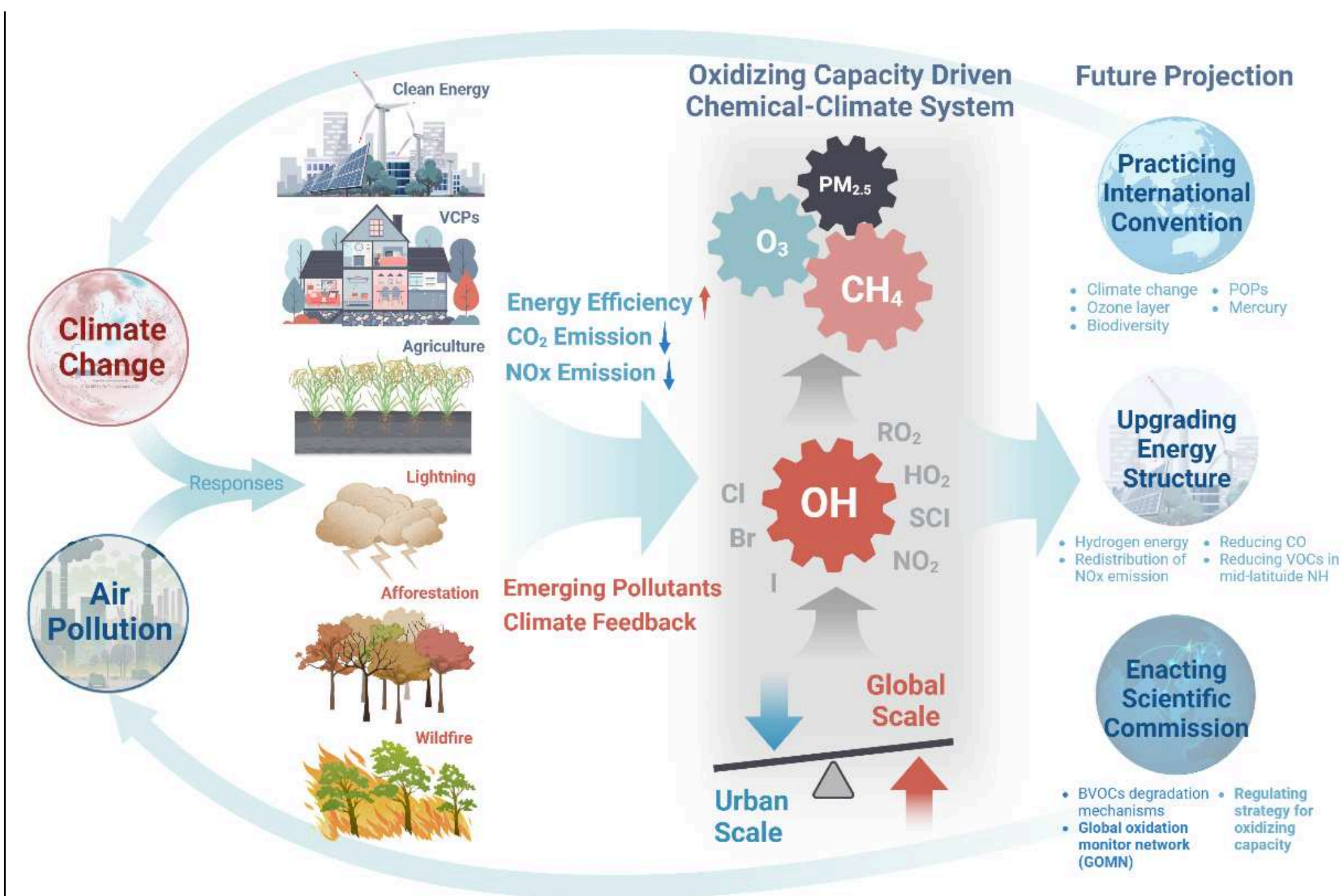
1033

1034 **Figure 2: Dependence of OH concentration and net ozone production rate**
 1035 **($P(O_3)$) on NO levels across marine, forest, and urban environments.**
 1036 Simulations were conducted using a chemical box model incorporating the
 1037 RACM2-LIM1 mechanism, which has been validated against field campaigns²⁷.
 1038 The principal distinction among the simulated environments lies in their VOC
 1039 compositions. VOC profile were derived from field observations at
 1040 representative locations: the tropical Atlantic Ocean (marine)²⁸, Amazon Forest
 1041 (forest)⁹⁷, and Beijing (urban)⁹⁸. In each scenario, VOC concentrations were
 1042 held fixed at observed levels, as were other trace gases and meteorological
 1043 parameters. Simulations were conducted under clear-sky, summer-like
 1044 conditions using daytime-averaged values (08:00-17:00 local time) and run for
 1045 one week to achieve steady state. To explicitly evaluate the NO dependence,
 1046 the observed NO concentration at each site was systematically scaled from
 1047 0.01 to 100 times the site-specific mean value (denoted by black dots). $P(O_3)$
 1048 represents the net ozone production rate, calculated as the difference between
 1049 gross ozone formation from NO oxidation by peroxy radicals and total oxidant
 1050 loss via ozone reactions with radicals and NO_2 . The detailed methodology for
 1051 this calculation has been described previously⁹⁹.



1052

1053 **Figure 3: Time series of annual mean OH concentrations for China, the United**
 1054 **States, and the global average, normalized to the year 2000.** OH
 1055 concentrations are derived from a 15-member initial-condition ensemble
 1056 simulation conducted with the Community Earth System Model version 2-Whole
 1057 Atmosphere Community Climate Model version 6 (CESM2-WACCM6). All
 1058 simulations used identical boundary conditions, with variations across
 1059 members resulting from perturbations in initial conditions³³. The model covers
 1060 the period 2000 to 2014 at a spatial resolution is $0.96^\circ \times 12.5^\circ$. The shaded
 1061 regions represent the range between the minimum and maximum values
 1062 across the ensemble members.



1063

1064 **Figure 4: A proposed framework for future decision-making from the**
 1065 **perspective of AOC.** The transition to carbon neutrality will substantially alter

1066 energy production and associated emission patterns. Simultaneously, natural
1067 emissions, such as those from biogenic sources, wetlands, and lightning,
1068 respond to ongoing climate change. The AOC critically influences the
1069 atmospheric lifetime of trace gases and the conversion of pollutants. To
1070 support effective regional air quality improvement, a scientifically grounded
1071 mitigation strategy should seek to regulate the AOC through balanced regional
1072 and global distribution.

1073 **Box 1: Global atmospheric composition responses to emission or boundary**1074 **condition perturbations.**

1075 Box 1 summarizes the projected response of global concentrations of CH₄, CO,
 1076 O₃, OH, and NO_x concentrations to minor perturbations in emissions or
 1077 boundary conditions. An upward arrow (↑) indicates a positive response, a
 1078 downward arrow (↓) a negative response, and a dash (-) no significant change.
 1079 In scenario a, reduced CH₄ emissions decrease atmospheric CH₄ levels and OH
 1080 consumption, leading to higher OH levels. In scenario b, although CO dominates
 1081 global OH turnover, CH₄ emissions exert a stronger influence on atmospheric
 1082 oxidation system because of their greater cumulative OH consumption (2.5 vs.
 1083 1 OH radical per molecule) and their role as the primary source of CO, making
 1084 CO emission perturbations comparatively minor²⁴. In scenario c and d, higher
 1085 NO_x concentrations generally enhance OH production on a global scale, thereby
 1086 shortening the atmospheric lifetimes of CH₄ and CO and reducing their
 1087 concentrations. However, atmospheric NO_x levels do not respond
 1088 proportionally to emission changes, and O₃ formation becomes relatively
 1089 insensitive to NO_x due to OH-mediated feedbacks. Scenario f involves
 1090 simultaneous reduction of CH₄, CO, and NO_x emissions by the same factor.
 1091 Scenario e and g represent enhanced ultraviolet radiation and elevated water
 1092 vapor, respectively, both promoting OH production via ozone photolysis. In
 1093 scenario h, elevated temperature perturbs atmospheric chemistry by
 1094 accelerating CH₄ oxidation (an OH-consuming process that reduces its
 1095 concentration), while also promoting OH production via ozone photolysis.

Initial change		Responses					
Scenario	Emission changes	CH ₄	CH ₄ lifetime	CO	O ₃	OH	NO _x
a	↓ CH ₄	↓	↓	↓	↓	↑	↓
b	↓ CO	-	-	↓	-	-	-

c	↑ NO _x	↓	↓	↓	-	↑	-
d	↓ NO _x	↑	↑	↑	-	↓	-
e	↑ Sunlight	↓	↓	↓	↓	↑	↓
f	↓ CH ₄ , CO, NO _x	↓	-	↓	↓	-	↓
g	↑ H ₂ O	↓	↓	↓	↓	↑	↓
h	↑ Temperature	↓	↓	-	-	-	-

1096

1097 **Box 2: Summary of measurement techniques and models for interpreting AOC**
1098 **for different scales.**

1099 On a global scale, the averaged OH concentration could be derived from the
1100 decay of the CH_3CCl_3 , whose lifetime is similar to that of CH_4 and thus an ideal
1101 substance to reflects the chemical sink of CH_4 . The production and emission of
1102 CH_3CCl_3 has ceased by early 2000s providing a clear decay trend to calculate
1103 the OH concentration for the last decade. However, the CH_3CCl_3 concentrations
1104 has recently dropped to below 5 pptv, substantially reducing the accuracy of
1105 OH estimates. It is therefore urgent and critical to identify an alternative to
1106 CH_3CCl_3 . An ideal alternative may be either a natural atmospheric component
1107 or an intentionally introduced compound, but it must satisfy the following
1108 criteria: well-defined sources, exclusive reactivity with OH radicals, an
1109 atmospheric chemical lifetime comparable to methane, and minimal adverse
1110 effects on human health or ecosystem. ^{14}CO is produced in the stratosphere
1111 from the interaction of cosmic rays with nitrogen (^{14}N). This ^{14}CO then diffuses
1112 into the troposphere and reaction with OH which is a major sink for CO in the
1113 atmosphere. As the lifetime of CO is only about a month, this method could
1114 provide hemispheric and continental OH concentrations with a time resolution
1115 of months. For regional and local scale, the metric of interest for AOC
1116 quantification shifts to the turnover rates of oxidations. This requires both the
1117 OH concentration and reactivity. Direct OH measurement can be achieved by
1118 laser-induced fluoresce or chemical ionization mass spectroscopy¹⁰⁰. The
1119 chemical reactivity of the airmass could be obtained by total OH reactivity
1120 measurements. These instrumentations could be equipped on ground-based or
1121 airborne platforms to provide local or regional AOC information. Here shows
1122 the summary of measurements techniques and models for interpreting AOC for
1123 different scales.

1124

Resolution Scale	Metric of interest	Requirement of measurements	Model	Possible improvement
Global	Decadal averaged [OH] for determining CH ₄ lifetime and background O ₃ production	CH ₃ CCl ₃	Earth system model	New tracers (natural or artificially added)
Continental	[OH] variation in the time scale of months	¹⁴ CO	Global model	Interactions between air pollution and climate change
Regional	Regional [OH]	Spatial-averaged measurement of regional OH concentration and total reactivity	Regional model	Vertical profile of oxidizing capacity, relation to secondary pollution
Local	[OH] and total OH reactivity to test against current chemical mechanism	In situ OH, total and speciated reactivity	zero-dimension model	Atmospheric flagship stations (comprehensive measurements of other oxidants and intermediates species, covering representative stations of forest, marine, urban), BVOCs degradation mechanisms, OH parameterization

1125